Hybrid MAC Protocol for Brain–Computer Interface Applications

Shams Al Ajrawi, *Student Member, IEEE*, Arafat Al-Dweik, *Senior Member, IEEE*, Ramesh Rao, *Fellow, IEEE*, and Mahasweta Sarkar, *Member, IEEE*

***Abstract*—Brain–computer interface (BCI) can permit individuals to use their thoughts as the sole means to control objects such as smart homes and robots. While BCI is a promising interdisciplinary tool, researchers are confronting network lifetime as an obstacle to further development. Furthermore, the medium access control (MAC) protocol is the bottleneck of the network reliability. There are many standards for MAC protocols that can be utilized for productive and dependable transmission by altering the control parameters. Modifying these parameters is another source of concern due to the scarcity in knowledge about its effect. In addition, there is no instrument accessible to receive and actualize these parameters on transmitters embedded inside the cerebrum. In this article, we give the transmission instrument to both ultrahigh-frequency (UHF) radio frequency identification (RFID) and ultra-wideband (UWB) signals for multiple transmitters and ultrasonic technology mimicking the neural dusts by modifying the superframe structure. In this article, a hybrid MAC protocol is proposed, and the results show that the traffic received can be increased by 700% for UHF-RFID and more than 100% for UWB and ultrasonic technology. Comparative results for wireless channel MAC protocols using these different transmission techniques are discussed in terms of network delay, data dropped, traffic sent, and traffic received.**

***Index Terms*—Brain–computer interfaces (BCIs), data dropped, delay, frequency-division multiple access (FDMA), medium access control (MAC), time-division multiple access (TDMA), ultrahigh-frequency radio frequency identification (UHF-RFID), ultrasonic, ultra-wideband (UWB).**

I. Introduction

BRAIN–COMPUTER interface (BCI) is a system that enables transmitting the human brain signals to an external device, which enables connecting the central nervous system of human beings with the external world [1]. One the objectives of BCI is to sidestep the damaged nervous system in the spinal cord and develop an immediate connection between the brain and an embedded device that can receive neural signals to imitate muscle function and, in so doing, overcome paralysis [2]–[5]. For example, individuals who are tetraplegic have normal neural signaling, however, suffer paralysis due to downstream damage at the spinal cord. BCI technology enables a functional cerebrum to communicate directly to computer-assisted devices that serve in place of muscles to re-establish functional movement. Using BCI, people can be prepared to rehearse contemplation to induce neural signals that can be deciphered by a computer [5]. As medical technology is exponentially developing, BCI stands at the forefront of personalized and predictive medicine [6], [7]. Specialists are attempting to use BCI to create prosthetic arms for patients to have optimal control of motion and use the functional electrical stimulation device to reanimate paralyzed arms [7], [8].

A BCI is a system comprising a number of sensors, a neural decoder or translator, and some form of actuator to carry out an action. The sensors' main task is to detect changes in neural activity related to the intent to influence or move an external device. Generally speaking, sensors can be placed inside or outside the skull, and each approach has some advantages and disadvantages. For the case where sensors are placed outside the skull, noninvasive, the sensors' are simply attached to the scalp and connected using to the decoder using a simple set of wires. However, the signals detected by the sensors' in this case suffer from severe attenuation caused by the skull, scalp, and other layers that cover the brain. Embedding the sensors inside the skull, invasive, is more complicated because the sensors have to be surgically implanted on the surface or within the depth of the brain; nevertheless, it provides high-quality signals and allows fast data transfer. The sensors in this case should be equipped with a transmitter to allow sending the signal out of the skull and then acquired by a number of receivers attached to the scalp [9]. In such scenarios, enabling several embedded sensors to communicate with external receivers wirelessly requires establishing a wireless network to manage the communications process between the transmitters and receivers.

There are many factors that must be considered while designing BCI wireless networks, because of the stringent constraints on the power consumption and size of the communicating tags. Therefore, a large portion of the research work on invasive BCI focuses on the physical layer, as reported in [10] and the references listed therein. However, the medium access control (MAC) protocol may have significant impact on the power consumption of such networks, and hence, it is essential to design an efficient MAC that has high power efficiency while being capable of providing fast and reliable data transfer. In particular, when the number of sensors is large, optimizing the

Manuscript received November 15, 2019; revised August 31, 2020; accepted October 6, 2020. Date of publication October 28, 2020; date of current version June 16, 2021. *(Corresponding author: Arafat Al-Dweik.)*

Shams Al Ajrawi, Ramesh Rao, and Mahasweta Sarkar are with the Department of Electrical and Computer Engineering, San Diego State University, San Diego, CA 92182 USA (e-mail: salajraw@eng.ucsd.edu; rrao@ucsd.edu; msarkar2@mail.sdsu.edu).

Arafat Al-Dweik is with the Center for Cyber Physical Systems, Khalifa University, Abu Dhabi 127788, UAE, and also with the Department of Electrical and Computer Engineering, Western University, London, ON N6A 3K7, Canada (e-mail: dweik@fulbrightmail.org).

Digital Object Identifier 10.1109/JSYST.2020.3030474

MAC design becomes crucial, and thus, the MAC design for BCI applications is becoming a fertile research field [11]–[13].

A. Basic MAC Protocols

MAC protocols are generally needed to manage the communications of multiple users by allocating each user a certain transmission resources such as time or frequency. Broadly speaking, MAC protocols can be classified into following three categories.

1) Channelization protocols:
   a) frequency-division multiple access (FDMA);
   b) time-division multiple access (TDMA);
   c) code-division multiple access.
2) Random access protocols:
   a) aloha:
      i) pure aloha;
      ii) slotted aloha.
   b) carrier sense multiple access (CSMA):
      i) CSMA with collision detection;
      ii) CSMA with collision avoidance (CSMA-CA).
3) Controlled access protocols:
   a) reservation.
   b) polling;
   c) token passing.

Each protocol has certain advantages and disadvantages in terms of spectral efficiency, delay, reliability, overhead, and complexity. For example, FDMA has low complexity and overhead because it does not require synchronization among the users. However, it has low spectral efficiency due to the frequency guard bands. Unlike TDMA, FDMA is immune to system timing issues since the frequency band is reserved for the user for the entire duration of the transmission session. Therefore, timing adjustment is not critical, and fewer number of bits is required for synchronization and framing [14]. In FDMA, it is rare for the receiver to get information from more than one transmission source. One of the key limitations for FDMA is the maximum data rate, which is minimal. FDMA can be attractive for BCI systems due to its simplicity; however, power consumption should be reduced.

B. Related Work

BCI systems can be generally classified as wireless sensor networks (WSNs), wireless body area networks (WBANs), or wireless personal area networks (WPANs). Therefore, the MAC for such networks can be adopted for BCI. Examples for these MACs are the IEEE 802.15.1 and IEEE 802.15.4. However, the characteristics of the brain environment are different from such networks [15], [16], which leads to a modest performance when WSN, WBAN, or WPAN protocols are adopted for BCI [11], [17]. Such local area networks (LANs) are typically based on the IEEE 802.15.1 and IEEE 802.15.4 standards. Such protocols relatively offer low cost and low power consumption and do not require underlying infrastructure. Nevertheless, these protocols are designed to support low data rates. More specifically, the IEEE 802.15.4 can support very long battery life and has very low complexity.

TABLE I
MAC PARAMETERS FOR WBAN, BCI, AND WSNS

Attribute	WBAN	BCI	WSN
power Source	Low	Ultra Low	Low
Architecture	Star	Star	Mesh
Traffic	Burst	Regular	Burst
Applications	Healthcare	Prosthetic	Various
Form Factor	Wearable	Implantable	Medium
Transceiver	m-range	Cm range	m-range
Power	Ultra Low	Ultra Low	Low
MAC	CSMA/TDMA	TDMA	CSMA
Protocol	BT/Custom	Custom	BT/ZB
Link Establish	One-by-one	All-at-once	One-by-one
Sync	Periodic	Periodic	Algorithmic
Spatial Resolution	Several mm	A few mm	Several mm
Covered Area	Head	Cortex	On Body
Invasion	Medium	Medium	No
Freely Motion	No	Yes	No
Electrode type	Surface Scalp	MEA	-
Electrode Position	Over Scalp	Intra-cortical	-

BT: Bluetooth; ZB: Zigbee.

In spite of the 802.15.4 advantages, it may have poor performance in terms of power consumption, reliability, and delay, if the MAC parameters such as the back-off window size and maximum number of retransmissions are properly selected. In [18], the authors investigated this problem and proposed an adaptive MAC algorithm for minimizing the power consumption while guaranteeing reliability and delay constraints. The data traffic is considered unsaturated, which allowed using sleep/wake-up modes to minimize the power consumption.

Periodic listening, idle listening, additional control overhead, and collision are the main drivers of power consumption. To manage these issues, the authors in [19] consider the out-of-band wake up radio. Nodes switch into sleep mode when there is no information for transmission. When a tag has data, the wake-up radio transmits the control signal to the fundamental circuit for the wake-up and information transmission. Furthermore, the tag remains in sleep mode to save power. The authors do not provide any system for crisis occasions. A review of various MAC protocols and the IEEE 802.15.4 for WBANs can be found in [10], where a diagnostic model is presented using delay and throughput, which effects low power tuning and vitality minimization. Moreover, path loss analysis is given for in-body, on-body, and off-body correspondence. MAC parameters for different networks are summarized in Table I.

C. Motivation and Main Contributions

As can be noted from the literature survey, very little work has been devoted to design an efficient MAC for BCI applications. In such applications where the sensors are embedded inside the skull, some constraints such as limited power and end-to-end delay are critical. The limited power constraint is mostly due the small size of the embedded sensors, and time constraint is imposed by the maximum tolerated delay between the brain activity and neuroprosthetic device response [17]. The throughput, received data rate, and delay are essential to extract sufficient

information in order to translate the neural signals into a desired movement. Therefore, this article proposes a new protocol for BCI applications that mitigates such problems and enhance the network performance. The new protocol combines the benefits of FDMA that allows using multiple channels without interference and with high throughput, TDMA can avoid collisions using a scheduling algorithm based on the breath first search (BFS) approach and CSMA-CA to improve the throughput and reduce the power consumption by reducing the idle listening state introduced by the TDMA [20], [21]. Therefore, the proposed MAC is hybrid.

Although the data rates for certain BCI applications such as the P300-based BCI can be very low [22], there are other applications that are currently being investigated, where much higher data rates might be required. For example, Kaplan *et al.* [23] considered adapting the P300-BCI for gaming applications. Furthermore, it is shown in [24] that an electroencephalogram (EEG) signal might require about 85 kb/s in particular scenarios. Therefore, the need for high data rate support for BCI systems is a key enabler for future BCI applications.

Moreover, to the best of the authors' knowledge, there is no research in the open literature that investigates different transmission technologies and mechanisms for BCI-MAC protocols. Therefore, the goal of this article is to determine the suitable technology for developing BCI systems among UHF-RFID, UWB, and ultrasonic, as well as to develop an MAC protocol that addresses previous concerns of network delay, data dropped, and traffic send/receive.

The performance of the proposed system is evaluated in terms of throughput, data rate, and time delay. The hybrid system is evaluated using three different combinations FDMA+TDMA, FDMA+CSMA, and FDMA+TDMA+CSMA, for three technologies, which are UHF-RFID, UWB, and ultrasonic. The obtained results show that the proposed hybrid MAC outperforms all the individual MACs and can satisfy the requirements of BCI applications. The results are presented for several cases of using 12 and 100 tags. The results are obtained using Opent [25], which is a highly reliable simulation tool that is used by several industrial giants such as Cisco and AT&T. Nevertheless, developing a test bed will be targeted in our future work to capture all practical aspects. The main obstacle for developing a test bed in the time being is the lack of reliable development kits that can support such a system.

D. Article Organization

This article is organized into five sections. Section I introduces the current scope of BCI and the purpose of this article. Section II presents the BCI system model. Section III presents the proposed hybrid protocol. Section IV presents the numerical and simulation results. Finally, Section V concludes this article.

II. BCI System Model

This article considers a BCI system, where N_T transceivers on the brain surface to collect and transmit the EEG brain signals, and N_R transceivers are placed on the scalp to acquire the transmitted signals. The sensors used are semiactive, and they remain idle until they receive brain signals to transmit. The wireless network parameters for BCI are investigated using the MAC protocols of three different technologies, which are ultrahigh-frequency (UHF) radio frequency identification (RFID) [26], [27], ultra-wideband RFID (UWB-RFID) [28], [29], and ultrasonic technology mimicking the neural dusts by modifying the superframe structure[15], [30], [31].

TABLE II
Lags at Different Frequencies

Frequency (MHz)	915	920	930	940
Lag (ms)	1.5	2.0	2.2	3.3

To select the appropriate frequency bands, the FDMA is tested using four distinctive frequency channels with RFID parameters, which mimics the realistic circumstance of multiple transmitters placed on the human brain to transmit the neural signals captured from the implanted electrodes to a receiver placed on the scalp. Since the frequency scope of passive RFID is from 860 to 960 MHz and the center frequency is 915 MHz, the four frequency channels utilized are 915, 920, and 930 MHz. The receiver analog-to-digital converter sampling rate is 200 kHz, and the channels are inspected at rate of 50 kHz per channel. Initially, 103 samples are used to generate the modulating signal, which is considered as a sinusoidal signal to represent the brain reaction and behavior of each signal at various frequency slots. The information signal is modulated using amplitude shift keying and passed through the channel. At the receiver, the received signal is passed through limited band filters to reduce the interference. The lag of the signal from the transmitter to the receiver is computed, as shown in Table II, for four different frequencies. Because the lag of the 940-MHz band is much larger than 2 ms, it will not be considered suitable for BCI applications.

III. Proposed Hybrid Protocol

The hybrid protocol is designed by dividing the N_T sensors into a number of clusters, three in this article, where FDMA is used to assign a frequency band for each cluster. Within each cluster, TDMA is used to multiplex the users to avoid interference between the sensors of that cluster. Finally, CSMA-CA is used to reduce the waiting time for the sensors in each cluster and, hence, reduce the delay and increase the throughput. This design allows the use of multichannels to transmit and receive in full duplex mode [32]. Each tag wakes up upon receiving a brain signal, communicates with its neighbors in the cluster, and goes to sleep until the next signal arrives. The communication between tags is through request-to-send (RTS) and clear-to-send (CTS) ACK. Fig. 1 shows the general design for the hybrid MAC protocol, in which the brain signals collected by biosensors are divided into three clusters and delivered to one receiver. The frequency and band slot assignment is performed using the BFS algorithm described in Section III-A.

A. Scheduling Algorithm

In this article, it is assumed that one of the tags has sufficient computationally capability, and it is called the main tag, which is

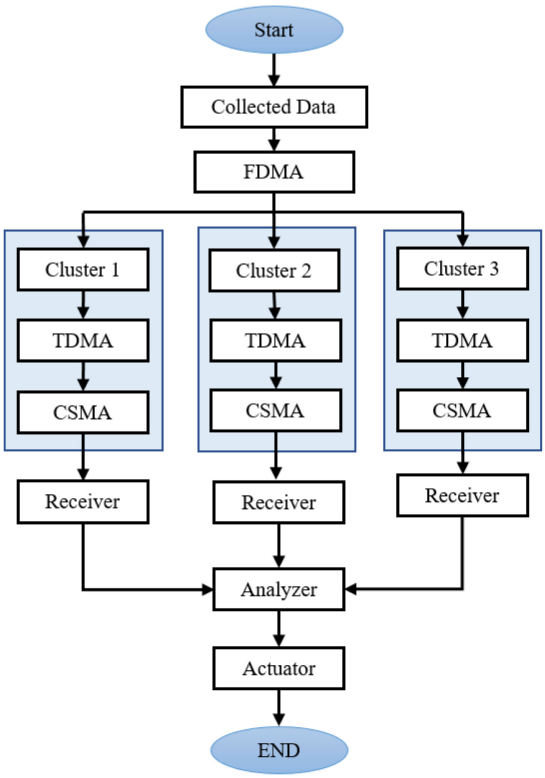

Fig. 1. Example of the hybrid MAC protocol using three FDMA channels and one receiver.

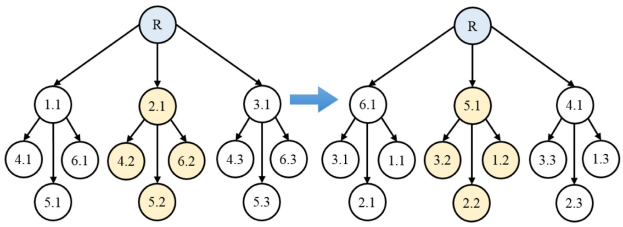

Fig. 2. Outcome of the first and second iterations of the scheduling algorithm using 12 tags, $T_{\text{Max}} = 6$.

used to construct the schedule for all the tags and implement the network connectivity graph that maximizes the network data rate and reduces the delay. Fig. 2 shows an example of the scheduling algorithm outcome using 12 sensing tags. In the figure, the circles represent the sensing tags; the first and second numbers represent the time slot and frequency band, respectively. The starting point is represented by a circle labeled with an R.

The BFS algorithm is used to assign a specific time slot and frequency band for each tag. Using BFS to implement the tree, the main tag serves as the root as we traverse through the tags. Therefore, the default time slot and frequency are assigned for each tag in the first level, and then, interference probability between one and two hops is checked. If there is a conflict between the N_j neighbor tags for N_i, we check the siblings. If they are in fact siblings, the algorithm assigns different time slots for N_i. The multichannel is used to send data to the same root tag (parent) at the same time slot using different assigned frequencies [33]–[35]. In the beginning, the default time slot is

Algorithm 1: Scheduling Algorithm.

Requirements: Biosensor Network Topology Graph
Graph: $G = (N, E)$
$N =$ set of 12 sensors
initialization
$N' = u$
for all tags N_i loop
  $Time\_Slot[u] \leftarrow current\_Time\_Slot$
  $Cluster\_Channel[u] \leftarrow 1$
    for all the same level visited 1-2-hop n of u **do**
      if ((Sub_Tree_parent[n] = Sub_Tree_parent[u]) OR(Number_of_Channels >= current_channels)) **then**
        if (Time_Slot[u] = $Time\_Slot[n]$) **then**
          $Time\_Slot[u] \leftarrow Time\_Slot[n] + 1$
        end if
      else
        if ((Time_Slot[u] = Time_Slot[n]) AND ($channel[u] = channel[n]$)**then**
          $channel[u] \leftarrow channel[n] + 1$
        end if
      end if
    end for
    for all not visited edge e of u **do**
    let L be the other not visited endpoint of edge e
      $Parent[L] \leftarrow u$
      $Height[u] \leftarrow Height[L] + 1$
    end for
end for

increased by one for the initial levels. Then, the time slots are updated to ensure that the time slot for the children tags is less than their parents. Therefore

$$T_{\text{New}} = T_{\text{Max}} - T_{\text{Current}+1} \tag{1}$$

where T_{New} represents the updated time slot, T_{Max} represents the total number of slots, and T_{Current} represents the currently assigned time slot. The scheduling algorithm is described in Algorithm 1.

The complexity of the scheduling algorithm, as described in [36]. Let $G(V, E)$ be a graph with $|V|$ number of vertices and $|E|$ number of edges. The BFS algorithm visits every vertex in the graph and every edge, where

$$\mathcal{O}(|V| + |E|). \tag{2}$$

B. Sender and Receiver Behavior

With the three clusters identified, each cluster is assigned a different channel, and when the cluster tags want to transmit simultaneously, the channel is checked periodically by the sensors. If sensor N_i sends an RTS control message to utilize its own time slot S_i to transmit a packet to a predefined receiver, and the channel is declared idle, i.e., the RTS and CTS have been communicated successfully between the tag and the receiver, then the tag sends the packet. However, if the CTS is not received by

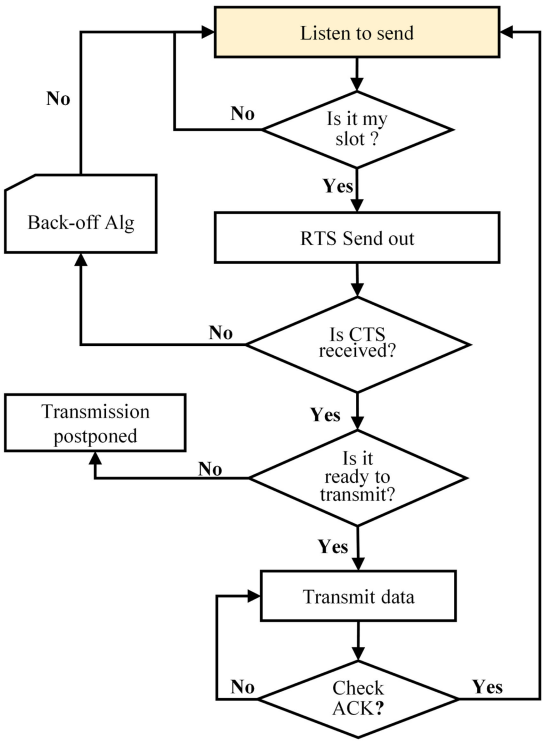

Fig. 3. Sender behavior.

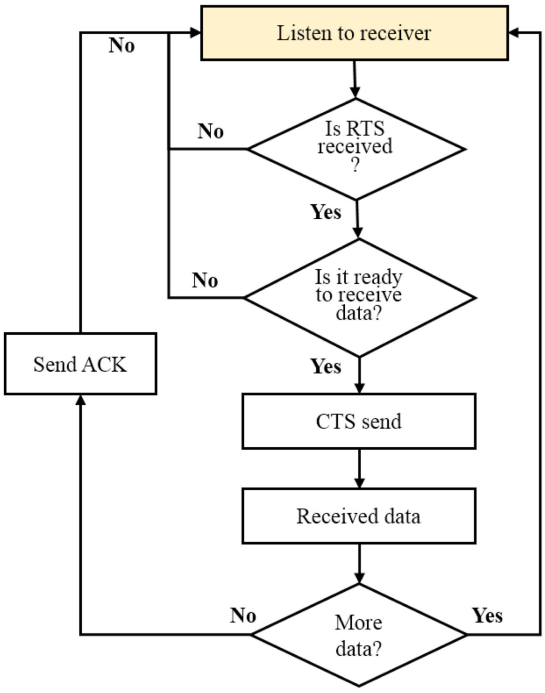

Fig. 4. Receiver behavior.

the sender, i.e., a collision occurred and transmission is inhibited to start the backoff algorithm to wait for a random number of frames, backoff delay, before next attempt to retransmit an RTS in the same slot. Figs. 3 and 4, respectively, show the sender and the receiver behavior for tag in a specific cluster to transmit data on an individually scheduled time slot.

TABLE III
NOTATIONS OF EQUATION PARAMETERS

Parameters	Description
T_{Fr}	Data time to end of frame
η	Throughput
T_{Oh}	Overhead time
T_{Sync}	Synchronization time
T_{Ta}	Turnaround time
T_{ACK}	ACK time
T_{GT}	Guard time
N_{Oh}	Overhead bits (total)
N_{ACK}	ACK/NACK bits
N_{Fr}	Data bits per frame
T_{BP}	Back-off period
T_{RTS}	RTS
T_{CTS}	CTS
T_{ITS}	Inter Frame Space
N_{Bo}	Number of back-off slots
T_{Bo}	Back-off slots' time
R_B	Data rate
D	Transmission Delay
C_L	Duty-cycle length
N_P	Number of packets
N_T	Number of tags
Q	Queue length
N_{Sync}	Number of synchronization bits
D_{EtE}	End-to-end delay
N_{TC}	Number of tags per cluster

C. Delay and Throughput of Various MAC Protocols

1) FDMA: The transmission delay for FDMA data can be computed as [37]

$$D_{\text{FDMA}} = T_{\text{Oh}} + T_{\text{ACK}} + T_{\text{GT}} + T_{\text{Ta}} + T_{\text{Fr}} \tag{3}$$

where $T_{\text{Oh}} = N_{\text{Oh}}/R_B$, $T_{\text{ACK}} = N_{\text{ACK}}/R_B$, and $T_{\text{Fr}} = N_{\text{Fr}}/R_B$. The throughput can be computed as

$$\eta = \frac{N_T N_P}{C_L}\left[1 + \frac{Q}{2(1-Q)}\right]. \tag{4}$$

where the notations are given in Table III.

2) TDMA: TDMA has three types of delays, which are transmission delay, queuing delay, and propagation delay. The transmission delay and for TDMA can be expressed as

$$D_{\text{TDMA}} = T_{\text{Oh}} + T_{\text{ACK}} + T_{\text{GT}} + T_{\text{Sync}} + T_{\text{Ta}} \tag{5}$$

where $T_{\text{Sync}} = N_{\text{Synch}}/R_B$. Therefore

$$\eta = \frac{N_P}{C_L}\left[1 + \frac{N_T}{2}\left(\frac{Q}{1-Q} + 1\right)\right]. \tag{6}$$

3) CSMA-CA: CSMA-CA works with the standard tag detecting medium by sending packets to the receiver when it finds that the medium is free. In the unlikely chance that the medium is occupied, the tag goes to random back-off time slots waiting for the channel to be free for transmitting. With the improved CSMA-CA RTS/CTS trade system tag that senses the free channel, it sends RTS to the receiver and waits for the CTS message from the receiver to start transmitting. The delay from

the sender to the receiver is calculated as

$$D_{\text{CSMA}} = T_{\text{Bo}} + T_{\text{Fr}} + T_{\text{Ta}} + T_{\text{ACK}} + T_{\text{ITS}} + T_{\text{RTS}} + T_{\text{CTS}} \tag{7}$$

where $T_{\text{BP}} = N_{\text{Bo}} T_{\text{Bo}}$. The relation between the transmission delay and throughput is given as

$$D_{\text{CSMA}} = \frac{(\kappa - 1)\left(\mathrm{e}^{2\eta} - 1\right)}{2 + 2D_{\text{EtE}} + 1} + 1 + D_{\text{EtE}}. \tag{8}$$

where κ is a metric used to capture the packet loss correlation on different links [37].

4) Hybrid MAC Protocol: For the hybrid model, the tags are divided into three clusters, and FDMA is used to assign a particular frequency band for each cluster. Within each cluster, the tags' data are multiplexed using TDMA and CSMA-CA. The delay for each of the cluster tag is given by

$$D_{\text{Hybrid}} = \frac{1}{N_{\text{TC}}}(D_{\text{FDMA}} + D_{\text{TDMA}} + D_{\text{CSMA}}). \tag{9}$$

The throughput of the different considered types of MAC protocols is calculated while assuming that the information is moved from the sender to the receiver utilizing only one of the MAC protocol types. Because of the similarity between the sender and the receiver, there is no collision or packet loss due to buffer overflow. Moreover, the channel is assumed error free. In such scenarios, the throughput can be expressed as [37]

$$\eta = 8\frac{T_{\text{Fr}}}{D} \tag{10}$$

where D is the total delay. Throughput calculated using (10) confirms that the proposed MAC protocol is preferable over other MAC protocols for BCI applications, as demonstrated by the presented numerical results.

D. Model Efficiency

Model efficiency can be calculated by considering transmission and propagation time for CSMA-CA by assuming that $M(t)$ is the number of full frames up to time t, as

$$\sum_{i=0}^{M(t)} T_f^i \le t \le \sum_{i=1}^{M(t+1)} T_f^i \tag{11}$$

$$\frac{1}{M(t)} \sum_{i=0}^{M(t)} T_f^i \le \frac{t}{M(t)} \le \frac{1}{M(t)+1} \sum_{i=1}^{M(t+1)} T_f^i \cdot \frac{M(t)+1}{M(t)} \tag{12}$$

where T_f is the frame time and T_f^i is X_i ith time frame, where the expected value of X_i is given by

$$\frac{1}{n}\sum_{i=1}^{n} X_i \to \mathbb{E}(x_i) \tag{13}$$

where $\mathbb{E}(\cdot)$ denotes the expectation process. Given that $t \to \infty$, then

$$\mathbb{E}(T_f) \le \frac{t}{M(t)} \le \mathbb{E}(T_f)\frac{1 + M(t)}{M(t)}. \tag{14}$$

On the other hand, the transmission efficiency can be expressed as

$$\zeta = \frac{M(t)T_t}{t} = \frac{T_t}{\mathbb{E}(T_f)} = \frac{T_t}{T_t + 2\mathbb{E}(N_{\text{Fa}})T_{\text{Pr}}} \tag{15}$$

where ζ is the transmission efficiency, T_t is the transmission time, and $E(N_{\text{Fa}})$ is the expected value for number of failed attempts, and T_{Pr} is the propagation time.

To calculate the expected value for the number of failed attempts, we consider that the first success happens at the nth transmission with probability

$$P_{S_1} = \frac{1}{e}\left(1 - \frac{1}{e}\right)^{n-1}. \tag{16}$$

Therefore, the expected value for the number of failed attempts is given by

$$\begin{aligned}\mathbb{E}(N_{\text{Fa}}) &= \frac{1}{e}\sum_{n=1}^{\infty}(n-1)\left(1 - \frac{1}{e}\right)^{n-1} \\ &= \mathrm{e} - 1.\end{aligned} \tag{17}$$

By plugging (17) into (15), we obtain

$$\zeta = \frac{T_{\text{Tx}}}{T_{\text{Tx}} + 2(\mathrm{e}-1)T_{\text{Pr}}} \tag{18}$$

where T_{Tx} is the transmission time. For $T_{\text{Tx}} \gg T_{\text{Pr}}$, it can be noted from (18) that $\zeta \to 1$.

IV. Numerical and Simulation Results

The network model used in this article follows the model given in [38]–[41], using three different RFID technologies, which are UHF, UWB, and Ultrasonic. For each technology, multiple tags are placed with parameters that mimic the implantable electrode array (MEA). For each technology, we evaluate the data dropped, network delay, and traffic sent/received for each case. The considered protocols are based on network time protocol [39], [40] concept, which provides synchronization and is used with both LANs and wide area networks (WANs).

The sensor properties are selected to match the network parameters such as the channel capacity, channel recurrence, transmit control, transmit power, receiver sensitivity, buffer size, and data rate. The results for the delay and throughput are calculated after feeding OpNet [25] simulation the interarrival time as constant 1 ms, traffic generation parameters, start time as constant 0, ON-state time as exponential with a value of 10^{-3}, and OFF-state time as 4×10^{-3}, packet generation arguments as uniform $(0.5, 1)$ packet size in byte and no segmentation, Beacon interval, back-off time in seconds, as 2×10^{-2}, maximum receive life time as 0.5 s, and buffer size as 5 kbyte. Furthermore, we use the constant network model, which is more suitable for BCI applications. Table IV shows the required parameters for each technology to simulate the network.

The considered and proposed protocols are evaluated using 12 and 100 tags, and using three receivers for both cases. For the 12-tag scenario, the total number of tags is divided into three clusters, each of which has three tags, and assigned a unique frequency band, which can be 915, 920, and 925 MHz [42].

TABLE IV
PARAMETERS USED FOR PROTOCOL SIMULATION

	RFID	UWB	Ultrasonic
Frequency	908 MHz 912 MHz 915 MHz	3.5 GHz 4 GHz 4.5 GHz	1.85 MHz 1.95 MHz 2.05 MHz
Bandwidth	250 KHz	499.2 MHz	30 KHz
Tx Power	0.2 mW	0.0026 mW	0.12 mW
Rx Sensitivity	-84 dBm	-85 dBm	-85 dBm
Buffer Size	5 kByte	5 kByte	5 kByte
Data Rate	2 Mbps	300 Mbps	1 Mbps

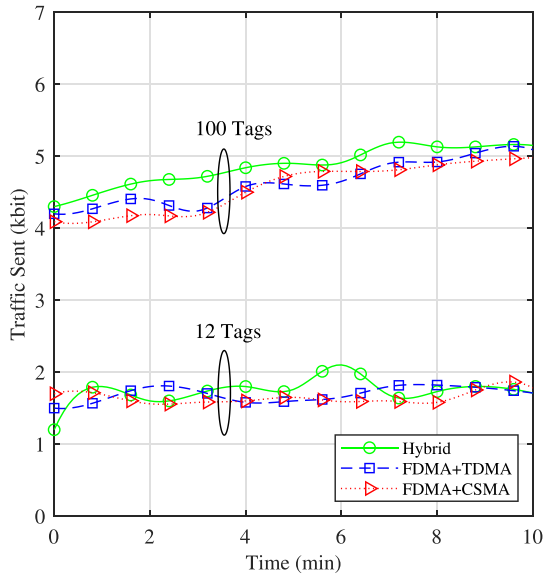

Fig. 5. UHF-RFID traffic sent using the hybrid, FDMA+TDMA, and FDMA+CSMA protocols for 12 and 100 tags.

The same argument is applied to the 100 tags, except that the three clusters contain 33, 33, and 34 tags. Then, three different protocols are applied as follows.

1) *FDMA+TDMA:* The tags send data over the three frequencies at different time slots to three receivers. Therefore, all the tags in a given cluster are assigned one out of available time slots, and thus, this protocol is denoted as FDMA+TDMA.
2) *FDMA+CSMA:* The tags in each cluster use CSMA-CA, and thus, two different tags in different clusters may transmit at the same time, but at different frequency, and hence, this protocol is called FDMA+CSMA. The starting time for the tags to transmit data is 10^{-2} s.
3) *Hybrid:* In this scenario, the tags in each cluster imply TDMA for multiaccess; however, CSMA is applied as well to allow tags that have data to transmit to utilize the time slots of the idle tags. Therefore, this protocol effectively composed of three protocols: FDMA+TDMA+CSMA.

Figs. 5–8 show traffic sent, traffic received, dropped data, and network delay for the proposed and other considered protocols using UHF. The x-axis represents the runtime of the simulation. For the 12-tag scenario, it can be noted that the three considered protocols can send roughly the same amount of data, but the

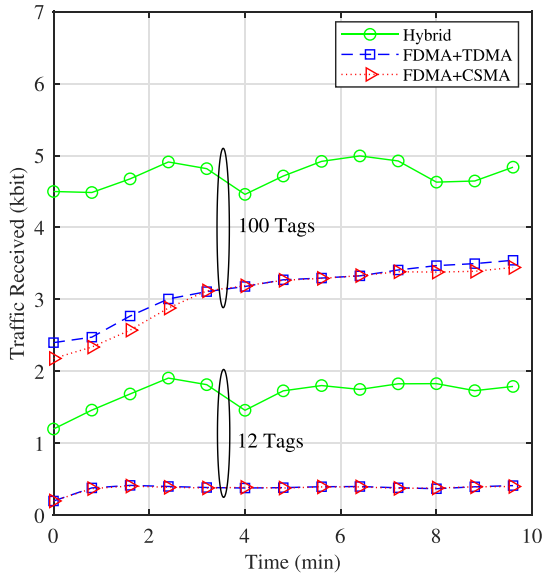

Fig. 6. UHF-RFID traffic received using the hybrid, FDMA+TDMA, and FDMA+CSMA protocols for 12 and 100 tags.

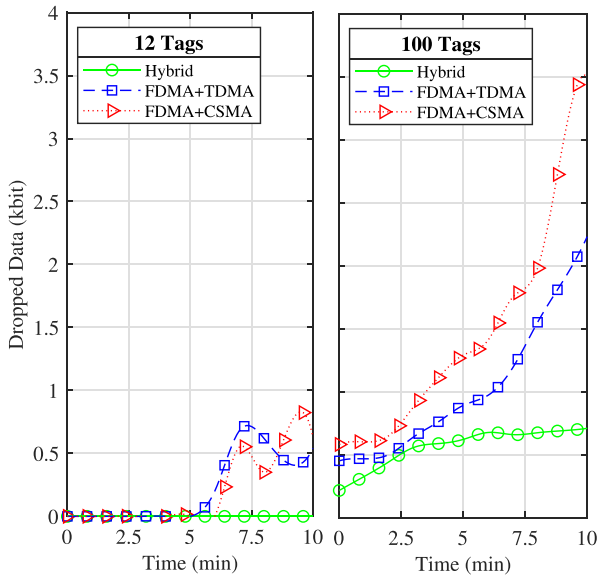

Fig. 7. UHF-RFID data dropped for the hybrid, FDMA+TDMA, and FDMA+CSMA protocols using 12 and 100 tags.

received data for the hybrid are significantly larger, because it suffered less dropped data. For the network delay, the hybrid protocol offers the minimum, while the other two protocols perform generally the same in all aspects. For the 100-tag scenario, it can be noted that the hybrid protocol can transmit slightly higher data, but the traffic received is significantly larger because the dropped data are much less. The traffic delay of the hybrid protocol is substantially less than the other two protocols. For the 100-tag scenario, it can be noted that the data sent increase over time as the buffer fills over time. Table V shows the numerical results for all the considered metrics. From these summarized results, it can be concluded that the hybrid protocol is the most compatible with brain function as observed by the previous

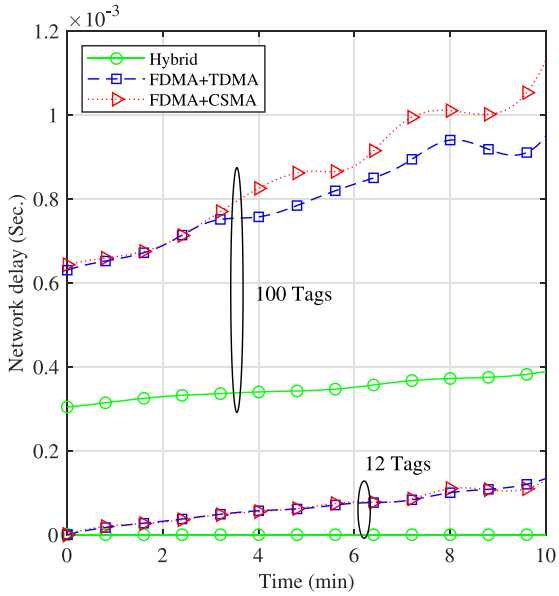

Fig. 8. UHF-RFID network delay for the hybrid, FDMA+TDMA, and FDMA+CSMA protocols using 12 tags and 100 tags.

TABLE V
UHF-RFID RESULTS USING 12 TAGS AT THE LAST SIMULATION POINT

Protocol	Tx Traffic (kbps)	Rx Traffic (kbps)	Dropped (kbps)	Delay (sec.)
FDMA+CSMA	1.8	0.24-0.38	0-0.6	0.15
FDMA+TDMA	1.5-1.78	0.24-0.38	0-0.6	0.15
Hybrid	1.2-1.8	1.2-1.8	0	0

reported research. From previous studies [11], the end-to-end time for the neural signal to travel from the action potential to the arm is nearly 60–90 ms. The hybrid protocol aligns with this previous knowledge as the delay is less than the BCI capturing time range and, therefore, suitable for BCI.

UWB radio technology supports microelectromagnetic systems. Circuit fabrication [18], [43] shows that for BCI applications, in order to capture the EEG signals by electrodes from inside the brain and transmit them wirelessly by a transmitter placed on the scalp to a receiver or processor located outside the skull, a transmission frequency of 3.5 GHz is used. Based on our last study, using 3.5 GHz gives better results in terms of the received signal strength, signal-to-noise ratio, path loss, and channel capacity [10], [44]. In Opnet, we used UWB parameters to transmit the data. We have implemented the different technologies in order to place the tags. The values for each tag were changed using edit attributes so that we can send the data packets according to the desired application. Generally speaking, for the brain space, the transmission of the data performs differently with UWB and RFID. The synchronization is performed by sending out beacon signals every 2×10^{-2} s. The first scenario analyzes transmitting the data with different frequencies at the same time. This method is similar to the frequency-division multiplexing in the CSMA-CA protocol. The frequencies used in this case are 3.5, 4, and 4.5 GHz. In this scenario, the tags begin to transmit data at 1×10^{-2} s.

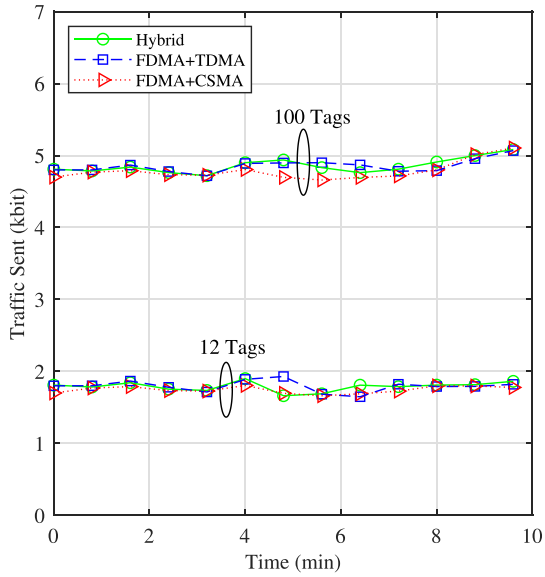

Fig. 9. UWB-traffic sent for three scenarios: hybrid MAC protocol, FDMA+TDMA, and FDMA+CSMA using 12 tags and 100 tags.

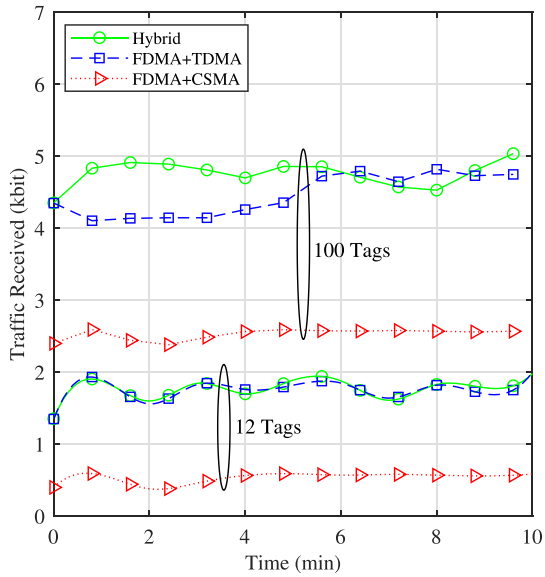

Fig. 10. UWB-traffic received for three scenarios; Hybrid MAC protocol, FDMA+TDMA, and FDMA+CSMA using 12 tags and 100 tags.

Figs. 9–11 present the network parameters for each of the three scenarios: FDMA+CSMA, FDMA+TDMA, and hybrid. As can be noted from Fig. 9, it can be noted that the buffering time is less significant as compared to the UHF as the traffic sent increase over time is very small. For traffic received, it can be noted that the hybrid and FDMA+TDMA significantly outperform the FDMA+CSMA. For the network delay depicted in Fig. 11, the delay for the 12 tags is very small and comparable for the three protocols. However, for the 100-tag case, it can be noted that the hybrid noticeably outperforms the other two protocols.

It is worth noting that the dropped data are zero for all protocols, and thus, the figure is not included. By considering

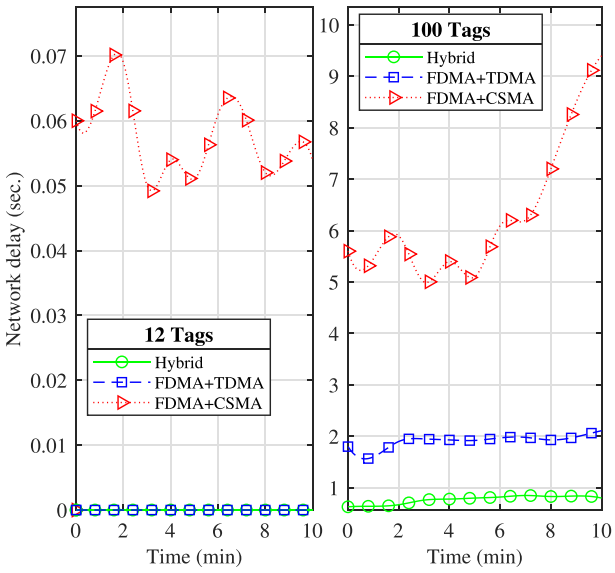

Fig. 11. UWB-network delay for three scenarios: hybrid MAC protocol, FDMA+TDMA, and FDMA+CSMA using 12 tags and 100 tags.

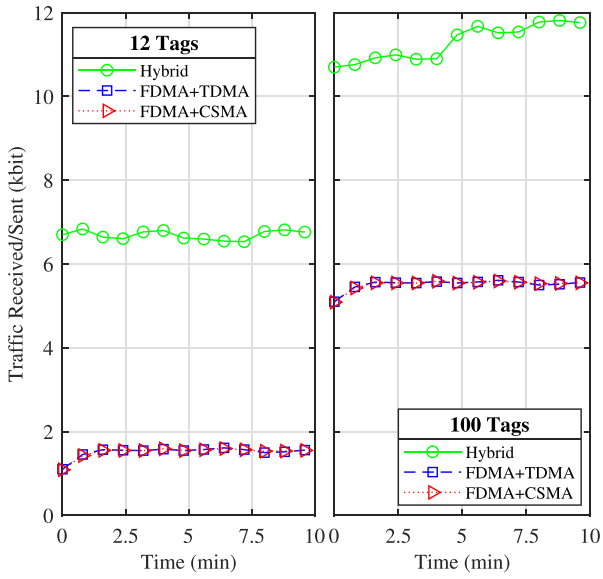

Fig. 12. Ultrasonic traffic sent or received for the hybrid, FDMA+TDMA, and FDMA+CSMA MACs using 12 and 100 tags.

TABLE VI
UWB SIMULATION RESULTS USING 12 TAGS

Protocol	Tx Traffic (kbps)	Rx Traffic (kbps)	Dropped (kbps)	Delay (sec.)
FDMA+CSMA	1.8	0.5	0	6×10^{-2}
FDMA+TDMA	1.2-1.8	1.2-1.8	0	0
Hybrid	1.6	2.1	0	0

this aspect, it can be concluded that the hybrid protocol works better for UWB technology. Table VI provides a comparison of the three scenarios. It can be noted that the hybrid protocol is the most compatible with natural brain function as the delay is within this limit for several cases of interest.

While ultrasonic has been used in medicine for many decades, it has only recently taken specialized form in bioelectronics, where promising new technology is developing. Ultrasonic has a potential for widespread use due to its ability to potently deliver power [45]. The smaller size of an ultrasonic transducer is an added advantage for applications such BCI. In Opnet, the ultrasonic technology parameters [29] were used to transmit data. The simulation is performed using the same procedure as described for the UHF and UWB. In the first scenario, the FDMA+CSMA protocol combines both FDMA and CSMA protocols. The tags transmit at different frequencies and detect the medium before transmitting data to avoid collisions. Each of the three clusters transmits at 1.85, 1.95, and 2.05 MHz, respectively [30]. The tags start transmitting data at 0 s. In this scenario, collisions are introduced early in the network; however, CSMA-CA is used to effectively avoid collisions [46].

In the second scenario, the FDMA+TDMA protocol calls for the network to include three clusters that use the same frequencies of the FDMA+CSMA and different times for transmission. For each cluster, one tag is designed to transmit any given time.

In the third scenario, the hybrid protocol includes each cluster with different frequencies and times for each given cluster,

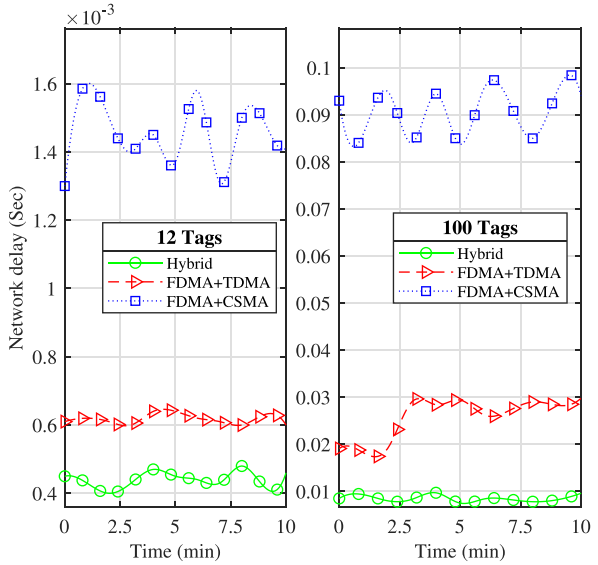

Fig. 13. Ultrasonic network delay for the hybrid, FDMA+TDMA, and FDMA+CSMA protocols using 12 and 100 tags.

similar to other two cases. However, each tag sends data only in a particular time slot. Three tags, one from each cluster, may send data in the same time slot. In order to prevent collision, the tag is forced to hold transmission for a random number of slots. Synchronization of all tags in each protocol is achieved by configuring the access point to broadcast beacon signals.

In Figs. 12 and 13, the network parameters are presented for each protocol. As can be noted from Fig. 12 for the 12-tag scenario, the hybrid protocol traffic sent/received is between 6.35 and 6.85 kb, the data dropped are approximately zero, and the network delay is about 4.2×10^{-4} s. For the FDMA+TDMA protocol, traffic sent and received was between 1.4 and 1.6 kb/s, and there were no data dropped. The network delay is between

TABLE VII
ULTRASONIC SIMULATION RESULTS USING 12 TAGS

Protocol	Tx Traffic (kbps)	Rx Traffic (kbps)	Dropped (kbit)	Delay (sec.)
FDMA-CSMA	1.5	1.5	0	1.6×10^{-3}
FDMA-TDMA	1.4-1.6	1.4-1.6	0	6.2×10^{-4}
Hybrid	6.35-6.85	6.35-6.85	0	4.2×10^{-4}

6×10^{-4} and 6.5×10^{-4} s. For the FDMA+CSMA protocol, the traffic sent was approximately 1.50 kb/s, the traffic received is about 1.45 kb/s, and the network delay is about 1.5×10^{3} s. Consequently, the hybrid protocol performs very well for this technology as well. For the 100-tag case, it can be noted that the delay becomes more critical for the FDMA+CSMA scenario, while it remains below 10^{-3} for the hybrid MAC. Table VII summarizes the results for each protocol in terms of traffic sent, traffic received, data dropped, and delay for the ultrasonic transmission using 12 tags. From the results, it is clear that the hybrid protocol performs better in terms of delay and data transmitted/received.

V. CONCLUSION

This article presented a new MAC protocol for BCI applications. The proposed MAC is based on combining three conventional MAC protocols to improve the transmission efficiency and reduce the delay. The proposed hybrid protocol divides the sensors into clusters, where the tags in a particular cluster are assigned a specific frequency band. The tags within each cluster use TDMA; however, the time slots can be accessed by other tags to reduce the average waiting time and, thus, reduce the delay and increase the throughput. The proposed hybrid protocol was compared with two other hybrid protocols, but only using a combination of two protocols. The obtained results demonstrated that the proposed hybrid MAC has several advantages in terms if delay, throughput, and dropped data. Moreover, specifically, the delay was significantly less than the other considered protocols, which makes it attractive for time-sensitive applications such as BCI.

REFERENCES

[1] Y. Cui *et al.*, "Identifying brain networks at multiple time scales via deep recurrent neural network," *IEEE J. Biomed. Health Inform.*, vol. 23, no. 6, pp. 2515–2525, Nov. 2019.

[2] J. Wolpaw and E. Wolpaw, *Brain-Computer Interfaces: Principles and Practice*. New York, NY, USA: Oxford Univ. Press, 2012.

[3] M. Al Ameen, N. Ullah, M. S. Chowdhury, S. Islam, and K. Kwak, "A power efficient MAC protocol for wireless body area networks," *EURASIP J. Adv. Signal Process.*, vol. 2012, no. 1, 2012, Art. no. 33.

[4] S. Katsigiannis and N. Ramzan, "DREAMER: A database for emotion recognition through EEG and ECG signals from wireless low-cost off-the-shelf devices," *IEEE J. Biomed. Health Inform.*, vol. 22, no. 1, pp. 98–107, Jan. 2018.

[5] E. Hodkin *et al.*, "Automated FES for upper limb rehabilitation following stroke and spinal cord injury," *IEEE Trans. Neural Syst. Rehabil. Eng.*, vol. 26, no. 5, pp. 1067–1074, May 2018.

[6] A. Javier, D. Leff, H. Yang, and G. Yang, "From wearable sensors to smart implants—Toward pervasive and personalized healthcare," *IEEE Trans. Biomed. Eng.*, vol. 62, no. 12, pp. 2750–2762, Dec. 2015.

[7] A. Fort, J. Ryckaert, C. Desset, P. Doncker, P. Wambacq, and L. Van Biesen, "Ultra-wideband channel model for communication around the human body," *IEEE J. Sel. Areas Commun.*, vol. 24, no. 4, pp. 927–933, Apr. 2006.

[8] A. Waziri, A. Schevon, J. Cappell, R. Emerson, G. McKhann, and R. Goodman, "Initial surgical experience with a dense cortical microarray in epileptic patients undergoing craniotomy for subdural electrode implantation," *J. Neurosurgery*, vol. 64, no. 3, pp. 540–545, 2009.

[9] Cleveland Clinic, Invasive EEG Monitoring. [Online]. Available: https://my.clevelandclinic.org/health/diagnostics/17144-invasive-eeg-monitoring, Accessed on: Sep. 8, 2020.

[10] Y. Zhang and G. Dolmans, "A new priority-guaranteed MAC protocol for emerging body area networks," in *Proc. 5th Int. Conf. Wireless Mobile Commun.*, 2009, pp. 140–145.

[11] J. Lalwani, A. Kumar, M. Sarkar, S. Mohanty, and S. Ahmed, "A comparative study of MAC protocols in brain-computer interface (BCI) applications," in *Proc. Int. Conf. Wireless Mobile Commun.*, 2017, pp. 1522–1527.

[12] H. Harikrishnan, M. Sarkar, S. Nagaraj, and A. Mihovska, "An experimental study of a novel MAC protocol using UHF-RFID passive backscatter modulation for brain computer interface (BCI) applications," in *Proc. IEEE Int. Black Sea Conf. Commun. Netw.*, Sochi, Russia, 2019, pp. 1–5.

[13] H. Harikrishnan, A. Sarkar, C. Paolini, and A. Mihovska, "Design and evaluation of a novel MAC protocol for multi implantable UHF-RFID transmitters in brain computer interface applications," *Wireless Telecommun. Symp.*, New York, NY, USA, 2019, pp. 1–7.

[14] N. Jain, S. R. Das, and A. Nasipuri, "A multichannel CSMA MAC protocol with receiver-based channel selection for multihop wireless networks," in *Proc. 10th Int. Conf. Comput. Commun. Netw.*, 2001, pp. 432–439.

[15] D. Seo *et al.*, "Ultrasonic beamforming system for interrogating multiple implantable sensors," in *Proc. 37th Annu. Int. Conf. IEEE Eng. Med. Biol. Soc.*, Aug. 2015, pp. 2673–2676.

[16] S. Ullah, H. Higgins, B. Shen, and K. Kwak, "On the implant communication and MAC protocols for WBAN," *Int. J. Commun. Syst.*, vol. 23.8, pp. 982–999, Jul. 2010.

[17] R. Chvez-Santiago *et al.*, "Propagation models for IEEE 802.15.6 standardization of implant communication in body area networks," *IEEE Commun. Mag.*, vol. 51, no. 8, pp. 80–87, Aug. 2013.

[18] P. Park, P. Di Marco, C. Fischione, and K. H. Johansson, "Modeling and optimization of the IEEE 802.15.4 protocol for reliable and timely communications," *IEEE Trans. Parallel Distrib. Syst.*, vol. 24, no. 3, pp. 550–564, Mar. 2013.

[19] V. B. Mišić and J. Mišić, "A polling MAC for wireless sensor networks with RF recharging of sensor tags," in *Proc. Queen's Biennial Symp. Commun.*, Kingston, ON, Canada, 2014, pp. 76–80.

[20] A. Tzamaloukas and J. Garcia-Luna-Aceves, "A receiver-initiated collision-avoidance protocol for multi-channel networks," *IEEE Infocom*, 2001, vol. 1, pp. 189–198.

[21] S. Ganeriwal, R. Kumar, and M. B. Srivastava, "Timing-sync protocol for sensor networks," in *Proc. 1st Int. Conf. Embedded Netw. Sens. Syst.*, 2003, pp. 138–149.

[22] T. Castermans *et al.*, "Optimizing the performances of a P300-based brain–computer interface in ambulatory conditions," *IEEE Trans. Emerg. Sel. Topics Circuits Syst.*, vol. 1, no. 4, pp. 566–577, Dec. 2011.

[23] A. Y. Kaplan, S. L. Shishkin, I. P. Ganin, I. A. Basyul, and A. Y. Zhigalov, "Adapting the P300-based brain–computer interface for gaming: A review," *IEEE Trans. Comput. Intell. AI Games*, vol. 5, no. 2, pp. 141–149, Jun. 2013.

[24] S. Movassaghi, M. Abolhasan, J. Lipman, D. Smith, and A. Jamalipour, "Wireless body area networks: A survey," *IEEE Commun. Surv. Tuts.*, vol. 16, no. 3, pp. 1658–1686, Third Quarter 2014.

[25] OPNET Network simulator. Accessed: Aug. 13, 2020. [Online]. Available: https://opnetprojects.com/opnet-network-simulator

[26] P. Rutul, P. Patel, J. Lalwani, M. Sarkar, and S. Nagaraj, "Investigating the feasibility of multiple UWB transmitters in brain computer interface (BCI) applications," in *Proc. IEEE 13th Int. Conf. Wearable Implantable Body Sens. Netw.*, San Francisco, CA, USA, 2016, pp. 236–241.

[27] P. Patel, M. Sarkar, S. Nagaraj, and K. Kushalad, "Channel modeling based on statistical analysis for brain-computer-interface (BCI) applications," in *Proc. IEEE Conf. Comput. Commun. Workshop*, 2016, pp. 320–321.

[28] S. Al Ajrawi, S. Mohanty, M. Sarkar, R. Rao, A. Mihovska, and H. Baweja, "Investigating feasibility of multiple UHF passive RFID transmitters using backscatter modulation," in *Proc. Int. Symp. Perform. Eval. Comput. Telecommun. Syst.*, Jul. 2017, pp. 558–563.

[29] S. Al Ajrawi, H. Bialek, M. Sarkar, R. Rao, and S. Ahmed, "Bi-directional channel modeling for implantable UHF-RFID transceivers in BCI applications," *Future Gener. Comput. Syst.*, vol. 88, pp. 683–692, 2018.

[30] D. Seo, J. Carmena, J. Rabaey, E. Alon, and M. Maharbiz, "Neural dust: An ultrasonic, low power solution for chronic brain machine interfaces," 2013, *arXiv:1307.2196*.

[31] D. Seo *et al.*, "Wireless recording in the peripheral nervous system with ultrasonic neural dust," *Neuron*, vol. 91, pp. 529–539, Aug. 2016.
[32] J. Elson, L. Girod, and D. Estrin, "Fine-grained networked time synchronization using reference broadcast," in *Proc. Symp. Oper. Syst. Des. Implementation*, 2002, vol. 36, pp. 147–163.
[33] J. Zhao and R. Govindan, "Understanding packet delivery performance in dense wireless sensor networks," in *Proc. 1st Int. Conf. Embedded Netw. Sens. Syst.*, 2003, pp. 1–13.
[34] G. Zhou, C. Huang, T. Yan, T. He, J. A. Stankovic, and T. Abdelzaher, "MMSN: Multi-frequency media access control for wireless sensor networks," in *Proc. 25th IEEE Int. Conf. Comput. Commun.*, 2006, pp. 1–13.
[35] H. Balakrishnan, C. Barrett, V. Kumar, M. Marathe, and S. Thite, "The distance-2 matching problem and its relationship to the MAC-layer capacity of ad hoc wireless networks," *IEEE J. Sel. Areas Commun.*, vol. 22, no. 6, pp. 1069–1079, Aug. 2004.
[36] N. Meghanathan, "A greedy algorithm for neighborhood overlap-based community detection," *Algorithms*, vol. 9, no. 1, p. 8, 2016.
[37] N. Javaid *et al.*, "Analyzing medium access techniques in wireless body area networks," *Res. J. Appl. Sci., Eng. Technol.*, vol. 7, no. 3, pp. 603–613, 2014.
[38] S. Marinkovic, C. Spagnol, and E. Popovici, "Energy-efficient TDMA-based MAC protocol for wireless body area networks," in *Proc. 3rd Int. Conf. Sens. Technol. Appl.*, Jun. 2009, pp. 604–609.
[39] D. Mills, "Network time protocol (version 3) specification, implementation and analysis," RFC 1305, 1992. [Online]. Available: https://tools.ietf.org/html/rfc1305
[40] L. Lamport, "Time, clocks and the ordering of events in a distributed system," *Commun. ACM*, vol. 7, pp. 558–565, Jul. 1978.
[41] T. Vamsi and J. Smith, "Hybrid analog-digital backscatter: A new approach for battery-free sensing," in *Proc. IEEE Int. Conf. RFID*, 2013, pp. 74–81.
[42] A. Sample and J. Smith, "Experimental results with two wireless power transfer systems," in *Proc. IEEE Radio Wireless Symp.*, 2009, pp. 16–18.
[43] P. Patel, M. Sarkar, and S. Nagaraj, "Ultra wideband channel characterization for invasive biomedical applications," in *Proc. IEEE 17th Ann. Wireless Microw. Technol. Conf.*, 2016, pp. 1–6.
[44] P. Patel, J. Lalwani, A. Kumar, M. Sarkar, and S. Nagaraj, "Tracking the behavior of UWB transmissions in invasive BCI applications," in *Proc. IEEE 13th Int. Conf. Wearable Implantable Body Sens. Netw.*, 2016, pp. 205–210.
[45] Y. Zhao, Y. Hao, A. Alomainy, and C. Parini, "UWB on-body radio channel modeling using ray theory and subband FDTD method," *IEEE Trans. Microw. Theory Techn.*, vol. 54, no. 4, pp. 1827–1835, Jun. 2006.
[46] F. Bouabdallah, C. Zidi, R. Boutaba, and M. Mehaoua, "Collision avoidance energy efficient multi-channel MAC protocol for underwater acoustic sensor networks," *IEEE Trans. Mobile Comput.*, vol. 18, no. 10, pp. 2298–2314, Oct. 2019.

Shams Al Ajrawi (Student Member, IEEE) received the master's degree in electrical computer engineering from the New York Institute of Technology, New York, NY, USA, in 2009. She is currently working toward the Ph.D. degree with the University of California, San Diego (UCSD), San Diego, CA, USA, and San Diego State University, San Diego, as a joint doctor program student.

In 2016, she joined the Department of Electrical and Computer Engineering, San Diego State University. She is an Associate Faculty with UCSD, University of San Diego, National University, California Miramar University, Alliant International University, San Diego Miramar College, MiraCosta College, Grossmont College, and California Institute of Art Technology. Her research interests include wireless network communication and brain–computer interface.

Arafat Al-Dweik (Senior Member, IEEE) received the B.Sc. degree in telecommunication engineering from Yarmouk University, Irbid, Jordan, in 1994, and the M.S. (*summa cum laude*) and Ph.D. (*magna cum laude*) degrees in electrical engineering from Cleveland State University, Cleveland, OH, USA, in 1998 and 2001, respectively.

From 1999 to 2001, he was with Efficient Channel Coding, Inc., Cleveland, where he was a Research and Development Engineer working on advanced modulation, coding, and synchronization techniques. From 2001 to 2003, he was the Head of the Department of Information Technology, Arab American University in Palestine. From 2003 to 2012, he was with the Communications Engineering Department, Khalifa University, Abu Dhabi, United Arab Emirates. From 2013 to 2014, he was an Associate Professor with the University of Guelph, Guelph, ON, Canada. Since 2016, he has been a Visiting Research Fellow with the School of Electrical, Electronic, and Computer Engineering, Newcastle University, Newcastle upon Tyne, U.K.. He is also a Research Professor and a member of the School of Graduate Studies, Western University, London, ON, Canada. He has authored more than 110 published papers and five issued U.S. patents. He has extensive editorial experience.

Dr. Al-Dweik is an Associate Editor for the IEEE TRANSACTIONS ON VEHICULAR TECHNOLOGY and *IET Communications*. He has received several research awards. He was a recipient of the Fulbright Scholarship.

Ramesh Rao (Fellow, IEEE) received the Ph.D. degree from the University of Maryland, College Park, MD, USA.

In 1984, joined the University of California San Diego (UCSD), San Diego, CA, USA. Prior to assuming his current post in 2001, he was the Director of UCSD's Center for Wireless Communications. He has authored more than 100 technical papers and contributed two book chapters and chaired the technical program of the 1997 International Conference on Universal Personal Communications.

Dr. Rao was the Publications Editor of the IEEE Information Theory Society. He is on the Board of Governors of the IEEE Information Theory Society. He also guest edited the IEEE JOURNAL OF SELECTED AREAS IN COMMUNICATIONS special issue on "Multimedia Network Radios," in December 1998.

Mahasweta Sarkar (Member, IEEE) received the B.S. degree (*summa cum laude*) in computer science and engineering from San Diego State University, San Diego, CA, USA, in 2000, and the M.S. and Ph.D. degrees in computer engineering from the University of California, San Diego, in 2003 and 2005, respectively.

In 2006, she joined the Department of Electrical and Computer Engineering, San Diego State University. She has worked previously as a Research Scientist with SPAWAR Systems Center, Point Loma, San Diego, and with Sun Microsystems. She is the Director of the Wireless Networks Research Group. She has been instrumental in setting up the National Science Foundation funded Wireless Multimedia Communication and Networks Laboratory in her department. Her research interests include wireless data networks.

Dr. Sarkar is a recipient of the "President's Leadership Award for Faculty Excellence" for the year 2010.